Biochimica et Biophysica Acta 1837 (2014) 1293–1304

Contents lists available at ScienceDirect

Biochimica et Biophysica Acta

journal homepage: www.elsevier.com/locate/bbabio

The bacterial-type [4Fe–4S] ferredoxin 7 has a regulatory function under photooxidative stress conditions in the cyanobacterium *Synechocystis* sp. PCC 6803

H. Mustila, Y. Allahverdiyeva, J. Isojärvi, E.M. Aro, M. Eisenhut [1,*]

Laboratory of Molecular Plant Biology, Department of Biochemistry, University of Turku, 20014 Turku, Finland

ARTICLE INFO

Article history:
Received 14 December 2013
Received in revised form 10 April 2014
Accepted 13 April 2014
Available online 26 April 2014

Keywords:
Bacterial-type ferredoxin
Photooxidative stress
Regulation
Chloroplast DnaJ-like protein
Synechocystis

ABSTRACT

Ferredoxins function as electron carrier in a wide range of metabolic and regulatory reactions. It is not clear yet, whether the multiplicity of ferredoxin proteins is also reflected in functional multiplicity in photosynthetic organisms. We addressed the biological function of the bacterial-type ferredoxin, Fed7 in the cyanobacterium *Synechocystis* sp. PCC 6803. The expression of *fed7* is induced under low CO_2 conditions and further enhanced by additional high light treatment. These conditions are considered as promoting photooxidative stress, and prompted us to investigate the biological function of Fed7 under these conditions. Loss of Fed7 did not inhibit growth of the mutant strain Δ*fed7* but significantly modulated photosynthesis parameters when the mutant was grown under low CO_2 and high light conditions. Characteristics of the Δ*fed7* mutant included elevated chlorophyll and photosystem I levels as well as reduced abundance and activity of photosystem II. Transcriptional profiling of the mutant under low CO_2 conditions demonstrated changes in gene regulation of the carbon concentrating mechanism and photoprotective mechanisms such as the Flv2/4 electron valve, the PSII dimer stabilizing protein Sll0218, and chlorophyll biosynthesis. We conclude that the function of Fed7 is connected to coping with photooxidative stress, possibly by constituting a redox-responsive regulatory element in photoprotection. In photosynthetic eukaryotes domains homologous to Fed7 are exclusively found in chloroplast DnaJ-like proteins that are likely involved in remodeling of regulator protein complexes. It is conceivable that the regulatory function of Fed7 evolved in cyanobacteria and was recruited by Viridiplantae as the controller for the chloroplast DnaJ-like proteins.

1. Introduction

Ferredoxins (Fed) are small electron carrier proteins containing an iron–sulfur cluster. They are important electron distributors in various electron transfer processes including photosynthetic light reactions. The plant-type Fed, Fed1 harboring a [2Fe–2S] center is the most abundant Fed in the cyanobacterium *Synechocystis* sp. PCC 6803 (hereafter *Synechocystis*) [1]. Fed1 functions as the primary soluble electron acceptor of the photosynthetic electron transfer chain transferring electrons from photosystem I (PSI) to $NADP^+$ via ferredoxin:$NADPH^+$ reductase (FNR) and is therefore essential for the viability of *Synechocystis* [1] and other cyanobacteria [2]. Furthermore, Fed1 is known to directly transfer electrons to a wide range of other proteins that are involved in nitrogen assimilation, glutamate synthesis, fatty acid metabolism and the thioredoxin system [1,3].

In addition to Fed1, *Synechocystis* has seven low abundant Fed-like proteins, Fed2–5 and Fed7–9. Five of these are plant-type Fed proteins: Ssl0020 (Fed1), Sll1382 (Fed2), Slr1828 (Fed3), Slr0150 (Fed4) and Ssl2559 (Fed5). Expression of the major *fed1* is positively and its closest homolog, *fed4*, negatively regulated by light intensity, whereas transcription of *fed2* appears to be controlled by glucose availability [1,4]. Moreover, expression of the *fed1* gene is reduced after treatment with hydrogen peroxide (H_2O_2) and heavy metals such as cadmium and selenate, which are toxic, partly because they stimulate oxidative stress [4].

Along with the five plant-type Fed proteins, *Synechocystis* employs three bacterial-type Fed: Sll0662 (Fed7 [5]) is predicted to contain a [4Fe–4S] cluster, Ssr3184 (Fed8) a [4Fe–4S] and a [3Fe–4S] cluster and Slr2059 (Fed9) two [4Fe–4S] clusters (prediction according to Pfam database [6]). The distinct functions of these [4Fe–4S] Fed in photosynthetic bacteria and their possible involvement in photosynthetic processes are

Abbreviations: Chl, chlorophyll; D1, reaction center protein subunit of photosystem II; DCMU, 3-(3′,4′-dichlorophenyl)-1,1-dimethylurea; DMBQ, 2,6-dimethyl-p-benzoquinone; Fed, ferredoxin; FNR, ferredoxin:$NADPH^+$ reductase; GL, growth light; HC, high CO_2; HL, high light; LC, low CO_2; PS, Photosystem

* Corresponding author at: Institute of Plant Biochemistry, Heinrich-Heine-University Duesseldorf, Universitaetsstrasse 1, 40225 Duesseldorf, Germany. Tel.: +49 211 81 10467; fax: +49 211 81 13706.

E-mail addresses: hmsile@utu.fi (H. Mustila), allahve@utu.fi (Y. Allahverdiyeva), jaheis@utu.fi (J. Isojärvi), evaaro@utu.fi (E.M. Aro), m.eisenhut@hhu.de (M. Eisenhut).

[1] Present address: Institute of Plant Biochemistry, Heinrich-Heine-University Duesseldorf, 40225 Duesseldorf, Germany.

http://dx.doi.org/10.1016/j.bbabio.2014.04.006
0005-2728/

poorly understood. In contrast to *fed1*, expression of *fed7* and *fed8* was found to be upregulated in response to H_2O_2 [4]. In accordance to this, Marteyn et al. [5] demonstrated that a *Synechocystis* inactivation mutant in *fed7* is more sensitive to both H_2O_2 and selenate (SeO_4) than the wild type (WT). It was suggested that Fed7 operates in protection against selenate via the thioredoxin reductase–glutaredoxins–ferredoxin (NTR–Grx1–Grx2–Fed7) crosstalk pathway, where electrons from PSI are transferred via Fed1 to ferredoxin–thioredoxin reductase catalytic chain (FTRc). FTRc passes the electrons to Fed7 and finally to Grx2 that reduces selenate to a non-harmful form [5]. In addition, microarray analyses showed that the *fed7* transcript is upregulated in response to low inorganic carbon (C_i) availability [7] and in response to iron limitation [8,9] while the abundant *fed1* is downregulated.

In this study we analyzed the role of the bacterial-type Fed7 in *Synechocystis* under photooxidative stress promoting conditions. The detailed physiological characterization of the knockout mutant Δ*fed7* demonstrated elevated chlorophyll *a* (Chl *a*) and PSI levels and reduced amount and activity of PSII under LC conditions with fortification by additional HL treatment. Using whole genome microarrays we detected impaired response of components of the carbon concentrating mechanism (CCM) and deregulation of the flavodiiron protein (Flv) mediated alternative electron valve, Flv2/Flv4, on transcriptional level. This photoprotective component was also reduced on protein level. The results suggest that Fed7 is involved in dealing with photooxidative stress conditions, such as combined LC and HL, probably as a regulatory element. We present and discuss a hypothetical model describing this regulatory function of Fed7 in *Synechocystis*. Furthermore, phylogenetic studies suggest that cyanobacterial Fed7 was presumably recruited as redox sensor domain in chloroplast DnaJ-like proteins in Viridiplantae.

2. Material and methods

2.1. Cyanobacterial strains and growth conditions

The glucose-tolerant WT strain *Synechocystis* sp. PCC 6803 and the Δ*fed7* mutant were cultivated in BG-11 medium [10] pH 7.5 at 30 °C under continuous photosynthetic photon flux density (PPFD) of 50 μmol photons m^{-2} s^{-1} (growth light, GL) or under 200 μmol photons m^{-2} s^{-1} of white light (high light, HL). Liquid cultures were shaken to assure continuous gas exchange and kept at high CO_2 (air enriched with 3% CO_2, HC) or at low CO_2 (ambient air with 0.039% CO_2, LC). The BG-11 agar plates and liquid cultures for Δ*fed7* were supplemented with kanamycin (50 μg ml^{-1}). Cultures used in experiments were not supplemented with antibiotics.

For RNA isolation *Synechocystis* cells (starting at $OD_{750} = 0.05$) were grown under HC and GL conditions for 2 days, diluted to $OD_{750} = 0.1$ and shifted to LC conditions either under GL or HL. Cells were harvested in logarithmic phase after 2 days. Shift to HC and HL condition was started by diluting the cells to $OD_{750} = 0.05$ and cells were harvested in logarithmic phase after 18 h. For biophysical, O_2 measurements and protein isolation cells were grown for 3–4 days under LC conditions either under GL or HL.

2.2. Mutagenesis

In order to construct the inactivation strain Δ*fed7*, the open reading frame (ORF) *sll*0662 and its surroundings were amplified from *Synechocystis* WT DNA by polymerase chain reaction (PCR) with *sll*0662 specific primers: forward primer 5′-AGCCGCAGTGGTGATTGA AC-3′ and reverse primer 5′-AGGTGGCGGGCATTATCAGTA-3′. The amplified *sll*0662 gene fragment was ligated into the pGEM-T vector (Promega). The kanamycin resistance gene (Km^R) from pUC4K plasmid was inserted into the *Sma*I restriction site in the coding region of *sll*0662 (see Fig. 2B). The resulting construct was used to transform *Synechocystis* WT cells. The transformants were segregated by gradually raising the concentration of kanamycin to 50 μg ml^{-1}. Complete segregation of the mutation was confirmed by PCR [11].

2.3. RNA isolation, cDNA synthesis and RT-qPCR

40 ml of exponentially growing culture was harvested by centrifugation at 5000 ×*g* for 6 min at 4 °C and the pellet was washed with ice-cold buffer containing 0.3 M sucrose and 10 mM sodium acetate (pH 4.5). Total RNA was extracted by hot-phenol method as described before by Tyystjärvi et al. [12]. Contaminating genomic DNA was removed by treating samples with 2 units DNase (TURBO DNA-free kit, Ambion). RNA concentration and purity were measured with a NanoDrop spectrophotometer (Thermo Scientific). RNA integrity was verified by agarose gel electrophoresis.

First strand cDNA was synthesized from 300 ng of purified RNA using the SuperScript III Reverse Transcriptase kit (Invitrogen) and random hexamer primers (Thermo Scientific). The generated cDNA was diluted threefold and 5 μl was used as template for RT-qPCR. The constitutively expressed gene *rnpB* encoding the RNA subunit of RNase P was used as a reference. The Real Time Quantitative PCR (RT-qPCR) was performed on a Bio-Rad IQ5 system using iQ SYBR Green Supermix (BioRad) as a triplicate for each RNA sample. Samples lacking reverse transcriptase or template were used as negative controls. Melting curve analysis was performed after 40 cycles of PCR for each run to ensure the specificity of the expected amplicon product. Primer pair 1 (5′-CAAAATGGGGACGATGAAG-3′and 5′-CAAATGGGGATTGATTTGC-3′) was used for detecting *fed7* transcript (Fig. A.1), and primer pair 2 (5′-CACGTGGCTCCCAATACTTT-3′ and 5′-GTAACCCAGGGGACGAATTT-3′) for verification of the Δ*fed7* mutant (Fig. A.1). For the *rnpB* gene the primers described in Pollari et al. [13] were used. The efficiencies of amplicon groups were estimated by using the LinRegPCR program [14]. The changes in gene expression relative to the control were calculated as described in Sicora et al. [15].

2.4. Microarray analysis

Genome wide gene expression profiling was performed at The Finnish DNA Microarray and Sequencing Centre (Turku, Finland). RNA integrity was assessed using a Model 2100 Bioanalyzer (Agilent Technologies). 10 μg of total RNA was processed for hybridization to Agilent 8x15K custom cyanobacterium *Synechocystis* sp. PCC 6803 array. The array contains 2–4 specific and nonoverlapping probes for each 3262 ORFs [7]. Microarrays were pre-processed using the "normexp" background correction method to avoid negative or zero corrected intensities, followed by between-array normalization using the quantile method to make all array distributions identical. Control probes were filtered and within-array replicate probe spots were averaged. Pairwise comparisons between groups were conducted using Linear Models for Microarray Data (Limma) package from Bioconductor software (http://www.bioconductor.org/). The false discovery rate of differentially expressed genes for control and mutant comparisons was based on the Benjamini and Hochberg method. Genes with statistically significant ($q < 0.05$) differences were considered as differentially expressed genes. Annotation of the genes was performed according to Cyanobase (http://genome.microbedb.jp/cyanobase/Synechocystis).

2.5. In vivo absorption spectra

In vivo absorption spectra were measured with a UV-3000 spectrophotometer (Shimadzu, Japan) from 400 nm to 800 nm with OD_{750} adjusted to 0.6.

2.6. Oxygen evolution measurements

Photosynthetic oxygen evolution was measured in vivo with a Clark type oxygen electrode and Oxygraph control unit (Hansatech) at 30 °C

under saturating white light of 1300 μmol m^{-2} s^{-1}. The cells were resuspended in fresh BG-11 medium and adjusted to Chl *a* concentration of 10 μg ml^{-1} or to OD_{750} = 3.5. The whole-chain photosynthetic electron transfer rates were measured in the presence of 10 mM $NaHCO_3$ and the PSII electron transfer rates were measured in the presence of 2 mM 2,6-dimethyl-*p*-benzoquinone (DMBQ).

2.7. Chl a fluorescence measurements and P700 oxido-reduction

Fluorescence emission spectra at 77 K of whole cells were measured by a USB4000-FL-450 (Ocean Optics) spectrofluorometer. 100 μl cells adjusted to a Chl *a* concentration of 7 μg ml^{-1} were frozen in liquid nitrogen. Excitation light was passed through an f/3.4 monochromator (Applied photophysics) set to 580 or 440 nm. The spectra were smoothed by a moving median with an 8-nm window and normalized to PSI emission peak at 725 nm.

The quantum yield of PSII, Y(PSII), and PSI, Y(PSI), donor side limitation of PSI, Y(ND) were recorded from light curves by DUAL-PAM-100 (Walz) at 30 °C. To measure maximum quantum yield of PSII (F_v/F_m) the cells (15 μg Chl *a* ml^{-1}) were dark-adapted for 10 min and supplemented with 10 μM 3-(3′,4′-dichlorophenyl)-1,1-dimethylurea (DCMU), an inhibitor of electron transport between the Q_A and Q_B sites in the PSII. 200 μmol photons m^{-2} s^1 actinic red light was applied for determination of the maximal level of fluorescence (F_m). In order to determine P_m value, a maximal change of the P700 signal from the fully reduced to the fully oxidized state, cells were illuminated with far-red light (75 W/m^2) for 10 s, and the saturating pulse (5000 μmol photons m^{-2} s^{-1}) was applied for 300 ms.

2.8. Protein isolation, electrophoresis, and immunodetection

60 ml cells were harvested after 3–4 days of growth under GL or HL. The cell pellets were resuspended in ice-cold washing buffer containing 50 mM Hepes-NaOH, pH 7.5 and 30 mM $CaCl_2$ and total cell extract as well as the membrane and soluble fractions of *Synechocystis* cells were isolated according to Zhang et al. [16].

Membrane protein complexes were analyzed by blue-native electrophoresis (BN-PAGE). The membrane samples were washed and solubilized according to Zhang et al. [17] with the exception of using 2% dodecyl-β-D-maltoside (DM) for solubilization. Samples were loaded on an equal protein basis of 80 μg per well in 4 to 10% acrylamide gradient gel. The BN gel was prepared as described by Kügler et al. [18] with modifications from Herranen et al. [19]. Electrophoresis was performed at 0 °C by increasing voltage gradually from 50 V up to 150 V during the 3.5 h run. The gel was destained by changing to colorless cathode buffer after half of the gel was covered with dye.

SDS-PAGE was applied to analyze denatured protein samples. Proteins were solubilized in Laemmli SDS sample buffer at room temperature for 2 h, and separated by 12% SDS-PAGE containing 6 M urea. The proteins were electrotransferred onto a polyvinylidene fluoride (PVDF) membrane (Immobilon-P, Millipore, USA) using a semidry apparatus, and immunodetected by protein-specific antibodies. Antibodies against Flv2, Flv3, Flv4, Sll0218, and D1 proteins were used as described earlier [16,17,20]. PsaB and Atpβ antibodies were purchased from Agrisera. The OCP antibody was kindly provided by D. Kirilovsky (Institut de Biologie et Technologies de Saclay, Gif sur Yvette, France).

3. Results

3.1. Expression of the bacterial-type ferredoxin Fed7 under photooxidative conditions

In *Synechocystis* the ORF *sll*0662 encodes a 15 kDa protein with high similarity to Fed. In contrast to the plant-type Fed it does not contain a [2Fe–2S] but a [4Fe–4S] cluster domain as it is typical for bacterial-type Fed. According to Marteyn et al. [5] the protein was named Fed7. Previous microarray results [7] indicated *fed7* as the only transcriptionally up-regulated Fed 24 h after shift from HC to LC conditions. We could likewise observe by RT-qPCR analysis a 2 fold increased *fed7* transcript accumulation (Fig. 1) 48 h after the shift of *Synechocystis* WT from HC to LC conditions and furthermore found that additional stress by increased light intensity enhanced the upregulation (2.3 fold) of *fed7* expression. Under HC conditions changes in light intensity did not significantly affect *fed7* transcription. These results provided first indication for a likely role of Fed7 under conditions that provoke photooxidative stress in *Synechocystis*, such as excess light and concurrent limited electron acceptor regeneration under LC and HL [17].

3.2. Generation and physiological characterization of Δfed7 mutant

In order to investigate the biological function of Fed7 we generated a single mutant in *fed7* by insertional mutagenesis (Fig. 2A). Full segregation of the obtained kanamycin resistant mutant strain Δ*fed7* was verified as shown in Fig. 2B. The mutant Δ*fed7* was further tested for the effect of the insertion on *fed7* expression. As shown in Fig. 1, we could not detect any full-length transcript.

To test the hypothesis that Fed7 is important under LC and HL conditions we first analyzed Δ*fed7* in terms of general traits such as growth, and pigmentation after LC and light intensity shift. The Δ*fed7* mutant grew comparable to the WT under all tested conditions (Fig. A.2). The dispensability of Fed7 under standard growth conditions was previously shown by Marteyn at al. [5] as well. However, the mutant appeared more yellowish under LC conditions, which was also reflected by an altered pigment composition. In vivo room-temperature absorption spectra (Fig. 3) demonstrated that the Chl *a* content was significantly elevated in Δ*fed7* compared to WT under LC conditions. While the WT downregulated the Chl *a* content under HL treatment, in the mutant cells this reduction was less distinct. In direct comparison Δ*fed7* cells contained significantly elevated (1.3 fold) Chl *a* levels, which could be alternatively demonstrated from methanol extracts (Fig. A.3). Besides Chl *a* also carotenoid levels increased in Δ*fed7* cells under LC conditions. On the contrary, phycobilins were less abundant in the mutant in response to LC and HL treatment. In combination, enhanced carotenoid and reduced phycobilin contents likely cause the LC dependent yellowish phenotype of Δ*fed7*.

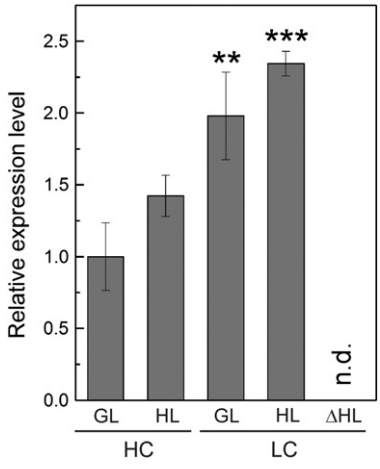

Fig. 1. Effect of C_i and light regimes on expression of *fed7* assessed by RT-qPCR. Relative transcription of the *fed7* gene is shown in response to shift from high CO_2 (3% CO_2 in air, HC) and 50 μmol photons m^{-2} s^{-1} (GL) to low CO_2 (0.039% CO_2 in ambient air, LC) for 48 h either at a PPFD of 50 μmol photons m^{-2} s^{-1} (GL) or 200 μmol photons m^{-2} s^{-1} of light (HL). In addition, fold change is shown after shift from HC and GL to HC and HL for 18 h. No *fed7* transcript was detected (n.d.) in the Δ*fed7* mutant (ΔHL). The results are the mean from three independent experiments ± SD (Student's *t*-test; $^{**}p < 0.01$; $^{***}p < 0.001$).

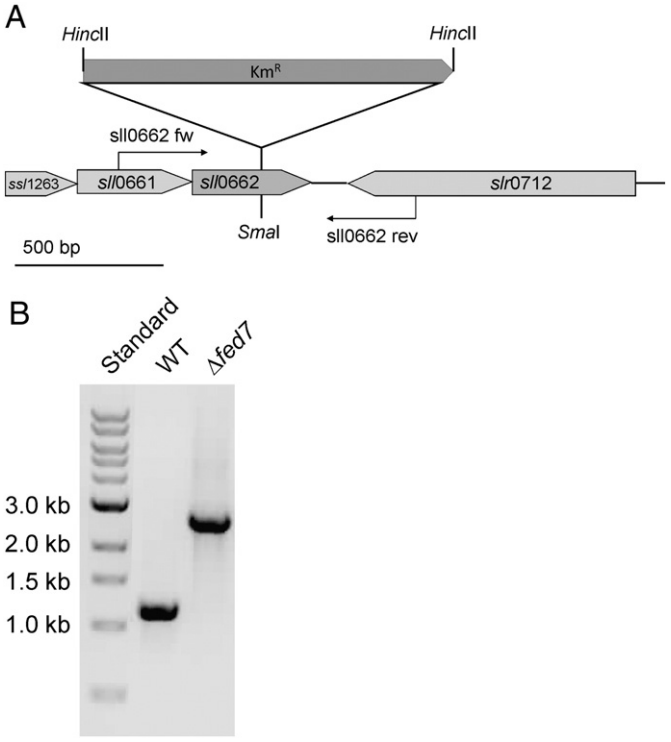

Fig. 2. Generation of Δ*fed7* mutant strain in *Synechocystis*. A, Strategy for the insertional inactivation of *fed7*. B, PCR analysis to verify full segregation of the Δ*fed7* mutant. Genomic DNA from WT and Δ*fed7* was used. The expected size of WT fragment is 1014 bp and mutant fragment 2262 bp. For more detailed information see Material and methods section.

3.3. Effect of Fed7 loss on photosynthesis

Plant-type [2Fe–2S] Fed mainly function in electron transfer processes connected with photosynthesis. Bacterial-type [4Fe–4S] Fed operate in various metabolic reactions in non-photosynthetic organisms. We assessed the question whether the biological function of the bacterial-type Fed7 in a photosynthetic bacterium is related to photosynthesis. Therefore, we studied photosynthetic parameters in the mutant and compared those to the WT.

3.3.1. Analysis of photosynthetic activity

To investigate possible effects of Fed7 deletion on the photosynthetic electron transfer rate we first measured O_2 evolution using a Clark-type electrode. Whole-chain electron transfer rates were determined using $NaHCO_3$ as electron acceptor. When samples were first normalized to equal cell numbers, WT and mutant cells were indistinguishable in their net photosynthesis rate under all tested conditions (Fig. 4A). However, when normalized to Chl *a*, net photosynthesis was reduced in the mutant under LC conditions. Approximately 70% activity under both light intensities could be monitored in Δ*fed7* compared to the WT (Fig. 4B).

For further dissection we assessed PSII and PSI properties separately. The analysis of O_2 evolution with DMBQ as artificial electron acceptor clearly showed that PSII functionality was negatively affected in Δ*fed7* under LC conditions only. Using same cell numbers, we recorded 10% reduction in PSII-dependent net photosynthesis in the mutant compared to WT (Fig. 4C). When we measured with equal Chl *a* amounts, the reduction was stronger. O_2 evolution declined to 88% and 77% in the mutant under LC and GL conditions, and was decreased to 68% upon LC and HL treatment (Fig. 4D).

By Chl *a* fluorescence measurements we determined lower F_v/F_m ratios in Δ*fed7* (Table 1), which indicated a reduced maximum quantum yield of PSII in the mutant upon LC and HL treatment. Also the effective quantum yield of PSII, Y(PSII), was lower in the mutant cells under increasing light intensities when compared with the WT (Fig. 4E, Fig. A.4A). To study PSI functionality we measured maximum oxidizable amount of P700, P_m, of LC grown cells (Table 1). The elevated P_m values pointed to increased PSI levels in the Δ*fed7* mutant. Additionally, we recorded light response curves of PSI quantum yield from cells either adapted to LC and GL or LC and HL conditions. In HL grown Δ*fed7* cells PSI quantum yield, Y(PSI), decreased and PSI donor side limitation Y(ND) increased at lower light intensities than in the WT (Fig. 4F). These differences could also be observed under GL conditions but to a lower extent (Fig. A.4B). Acceptor side limitation was not detected. The donor-side limitation of PSI in the mutant is consistent with the observed lower quantum yield of PSII, Y(PSII), since the low capacity of PSII does not match the enhanced capacity of PSI and may hence restrict PSI photochemistry (Fig. 4F).

3.3.2. 77 K fluorescence spectroscopy

To study changes in excitation energy transfer we recorded low-temperature (77 K) emission spectra of Δ*fed7* and WT upon either Chl *a* (λ = 440 nm) or phycobilin (λ = 580 nm) excitation in intact cells. Basically, under HC conditions the emission spectra of both strains did not differ (Fig. 5A, D).

Fluorescence emission spectra upon Chl *a* excitation showed the typical peaks at 690 nm and 725 nm, originating from PSII and PSI, respectively. The reduced peak at 690 nm demonstrated increased PSI/PSII ratio in Δ*fed7* after LC shift, which was enhanced by HL treatment (Fig. 5B, C).

Also the fluorescence emission spectra obtained after phycobilin excitation showed obvious differences under LC conditions only. Δ*fed7*

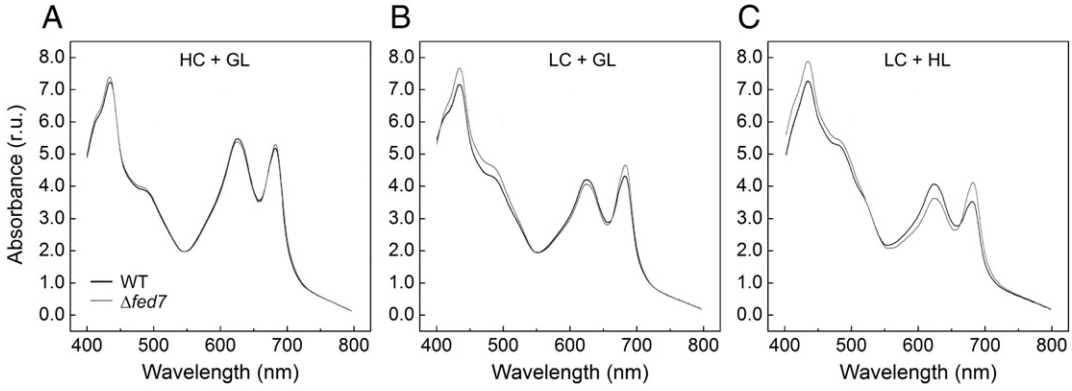

Fig. 3. In vivo room-temperature absorption spectrum of WT and Δ*fed7* cells in dependence on C_i concentrations and light intensities. Absorption spectra of *Synechocystis* cells grown for 3 days under HC (A) or LC (B–C) and under 50 (GL, A–B) or 200 (HL, C) μmol photons m^{-2} s^{-1}. Peaks at 485 nm, 625 nm and 678 nm derive from carotenoid, phycobilin and Chl *a*, respectively. Spectra were normalized at 750 nm.

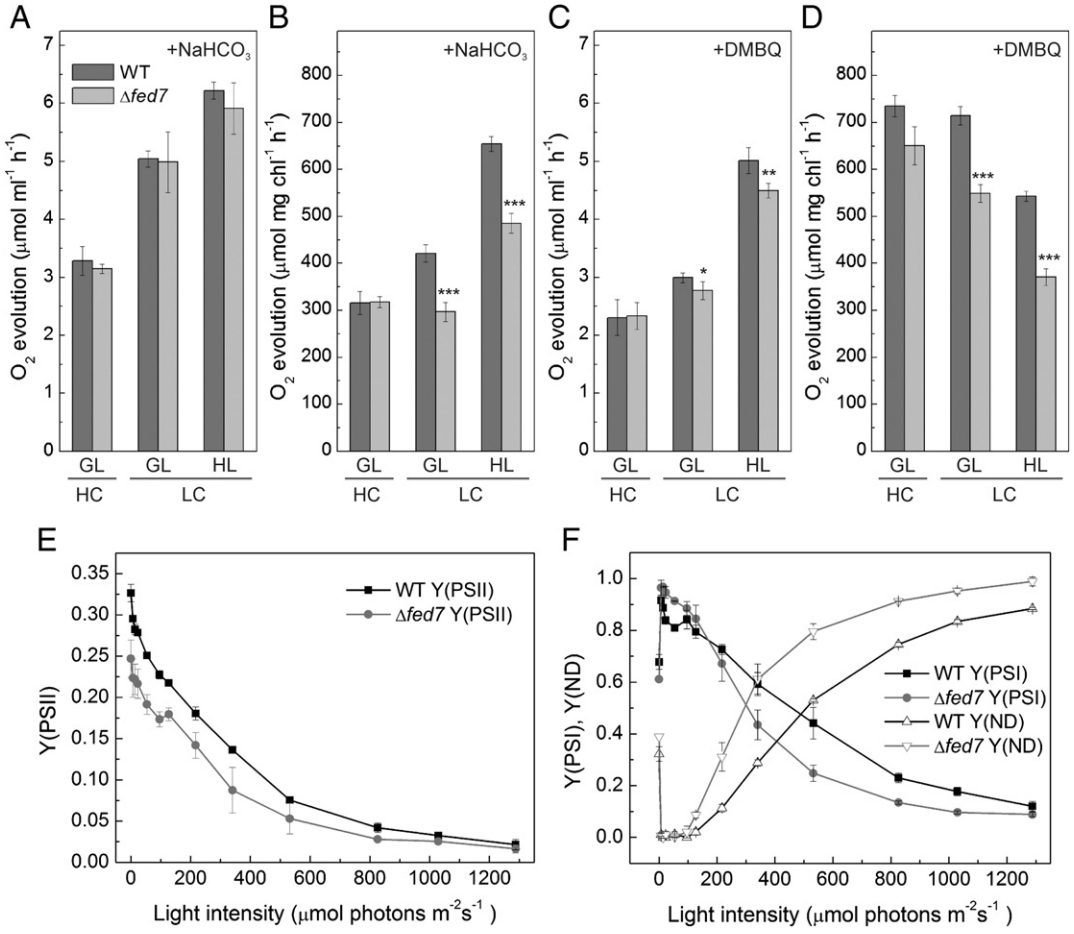

Fig. 4. Photosynthetic electron transfer and functional status of PSI and PSII. A–B, oxygen evolution rates of WT and Δ*fed7* mutant in intact cells in the presence of 10 mM $NaHCO_3$ and C–D, in the presence of 2 mM DMBQ. Cells were adjusted either to equal cell (A, C) or equal Chl *a* amount (B, D). E, effect of light intensity on quantum yield of PSII, Y(PSII) and F, the quantum yield of PSI (Y(PSI)) and donor side limitation (Y(ND)) of PSI in light adapted WT and Δ*fed7* cells grown under HL. Columns/curves and error bars represent means and standard deviation from three independent cultivation experiments (Student's *t*-test; $^{*}p < 0.1$; $^{**}p < 0.01$; $^{***}p < 0.001$).

cells grown under LC and GL conditions exhibited lower peak at 655 nm, which integrates the emission peaks at 645 nm and 665 nm of free phycobilisomes, and at 685 nm, the emission peak of terminal phycobilin emitters and PSII fluorescence [21] (Fig. 5E). After LC and HL treatment these reductions were pronounced (Fig. 5F). According to the results Δ*fed7* cells contained both reduced PSII and phycobilisome amounts.

3.3.3. Analysis of photosynthetic complexes on protein level

O_2 evolution, Chl *a* fluorescence analysis and 77 K fluorescence measurements indicated reduced PSII content and activity in the mutant. In order to further support the measured effects, also protein analyses were performed.

We conducted BN-PAGE analysis (Fig. 6) to study levels of the different thylakoid protein complexes. Basically, we observed that in Δ*fed7* cells PSII levels (monomers and dimers) were slightly reduced while PSI forms (monomers and trimers) were enriched in comparison to WT cells. In response to HL treatment the WT reduced PSII monomers and particularly PSI complexes, and accumulated PSII dimers. In the Δ*fed7* mutant the reduction of PSI complexes, especially PSI trimers (see BN-PAGE), was less stringent, while the decline in PSII complexes was stronger compared to WT upon HL treatment.

In accordance with the BN-PAGE analysis, also western blot analyses demonstrated changed total amounts of PSI and PSII center proteins. D1 levels were strongly reduced while PsaB contents did not show any difference in the Δ*fed7* mutant after LC and HL treatment when loaded on Chl *a* basis (Fig. A.5), since about 80% of all chlorophyll is associated with PSI. However, if loading was normalized according to total protein amounts (Fig. 7), D1 amounts in Δ*fed7* were only slightly lower than in WT cells after HL treatment. PsaB levels were clearly enhanced (app. 2 fold) in Δ*fed7* cells grown under both GL and HL. The outcome is that Δ*fed7* cells contained higher PSI and lower PSII levels under LC conditions leading to reduced PSII-dependent O_2 evolution (Fig. 4C, D) and increased PSI/PSII ratio in comparison to WT. HL treatment enhanced these effects.

Besides the photosystems itself we were also interested in possible changes of proteins involved in protection of these. Since we could show in an earlier work that the proteins Flv2 and Flv4 together with

Table 1
Fluorescence parameters of WT and Δ*fed7* cells grown under LC and different light regimes. F_0 and F_m were measured in the presence of 10 μM DCMU. P_m, a maximum oxidizable amount of P700, was measured after application of saturating pulse under far-red light background. Values are averages and standard deviation of three biological replicates.

		WT	Δ*fed7*
LC + GL	F_0	0.06 ± 0.002	0.06 ± 0.002
	F_m	0.12 ± 0.004	0.10 ± 0.004
	F_v/F_m	0.44 ± 0.005	0.41 ± 0.008
	P_m	0.11 ± 0.006	0.12 ± 0.005
LC + HL	F_0	0.10 ± 0.011	0.09 ± 0.007
	F_m	0.14 ± 0.013	0.11 ± 0.010
	F_v/F_m	0.28 ± 0.030	0.20 ± 0.007
	P_m	0.39 ± 0.022	0.47 ± 0.010

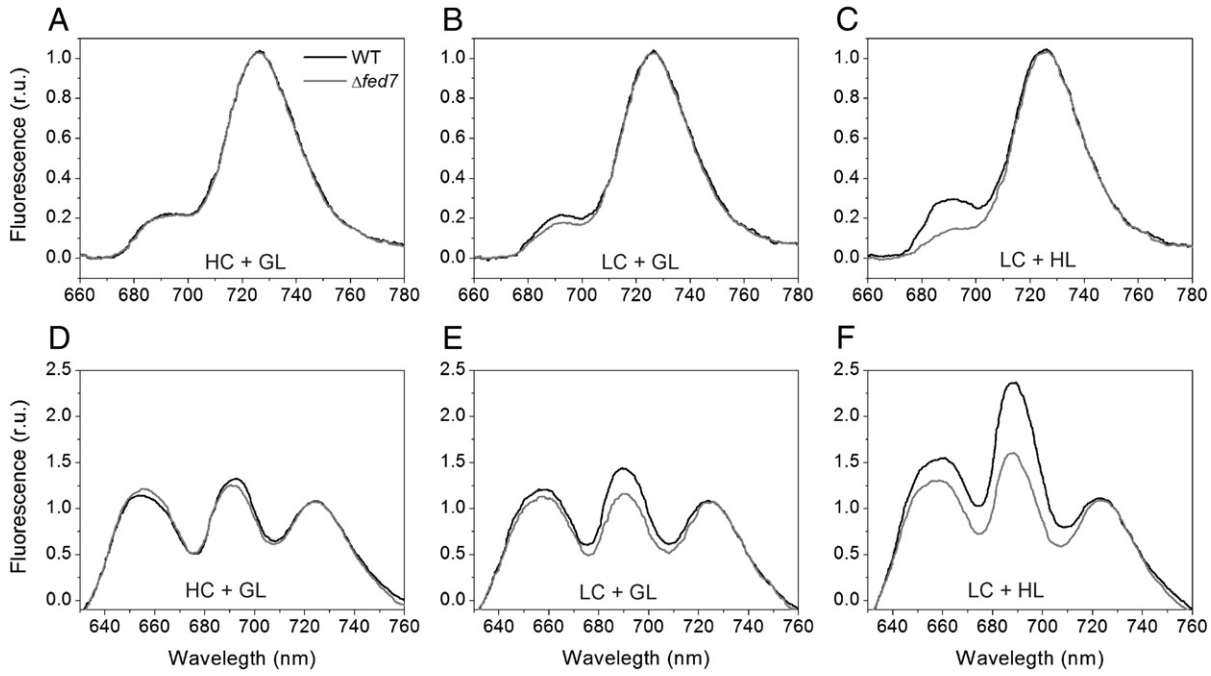

Fig. 5. Low-temperature fluorescence emission spectra of WT and Δ*fed7* cells grown under different C_i and light regimes. Spectra were recorded at 77 K from WT (black line) and Δ*fed7* (gray line) cells grown under HC (A, D) or LC (B–C, E–F) and under 50 (GL, A–B, D–E) or 200 (HL, C, F) μmol photons m^{-2} s^{-1}. A–C, Spectra with excitation of Chl *a* at 440 nm and D–F, spectra with excitation of phycobilins at 580 nm. Data were normalized to the PSI emission peak at 725 nm. Each spectrum represents an average of three independent liquid cultures.

Sll0218 provide *Synechocystis* with an important PSII photoprotective mechanism under photooxidative stress conditions [16,17], we also analyzed the accumulation of these proteins. Flv2, Flv4 and especially Sll0218 amounts were less in Δ*fed7* than in WT when incubated under LC and HL conditions (Fig. 7). In contrast, the amount of Flv3, which participates in the Mehler-like reaction [22–24] and is important in HL acclimation [25], was similar in both lines. Importantly, also levels of the orange carotenoid protein (OCP [26]), which functions in photoprotective non-photochemical quenching [27], were not changed in Δ*fed7* in comparison to WT (Fig. 7).

3.4. Identification of differentially expressed genes in Δfed7 mutant

The functional diversity of Fed is not only restricted to metabolic reactions but also includes redox regulation on enzymatic and transcriptional level. We performed microarray analysis to investigate possible implications of loss of Fed7 on gene expression and searched for alterations in transcript abundances between Δ*fed7* and WT under LC conditions.

In summary, we found 54 genes significantly ($q < 0.05$) upregulated (Table 2) and 68 genes significantly downregulated in Δ*fed7* (Table 3) compared to WT 48 h after shift from HC to LC conditions. The light intensity (here: GL) remained unchanged. Most of the up-regulated transcripts encode proteins of unknown function. However, we identified one gene that is involved in a final step of Chl *a* biosynthesis. The gene *slr*0750 (2.2 fold) encodes the light-independent protochlorophillide oxidoreductase (ChlN), which catalyzes the reduction of protochlorophyllide to the Chl precursor chlorophyllide [28]. In addition, the transcription of *slr*0749 (ChlL), functioning in the same pathway as ChlN [28], and *ssr*1251 (hypothetical protein), encoded from the same chromosomal region as ChlN, was also enhanced. The enhanced expression of these Chl *a* biosynthesis genes might be the reason for the elevated Chl *a* content in Δ*fed7*. Interestingly, also *slr*0090 is stronger expressed in Δ*fed7* than in the WT (1.6 fold). The gene encodes 4-hydroxyphenylpyruvate dioxygenase (HPPD), which is essential for

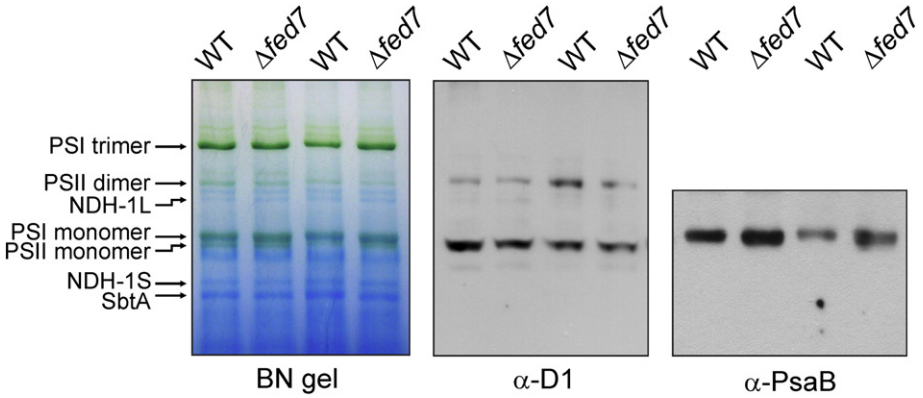

Fig. 6. Changes in thylakoid protein complexes in WT and Δ*fed7* cells grown at LC and different light regimes. Samples were harvested from cultures grown under LC plus GL and HL conditions, respectively. Proteins were separated by BN-PAGE, transferred onto PVDF membrane and immunodetected using specific antibodies. Thylakoid membrane protein complexes (80 μg of protein per sample) were solubilized with 2% (w/v) DM prior to BN-PAGE. The protein complexes in the BN-gel were identified according to Herranen et al. [19].

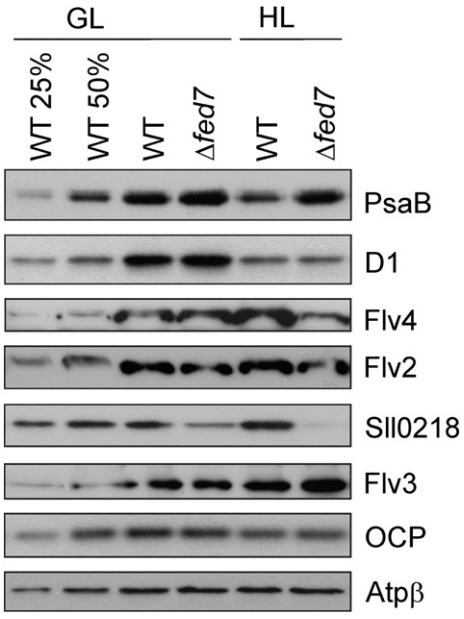

Fig. 7. Changes in protein abundance in WT and Δ*fed7* cells grown at LC and different light regimes. Samples were harvested from cultures grown under LC plus GL and HL conditions, respectively. Proteins were separated by SDS-PAGE, transferred onto PVDF membrane and immunodetected using specific antibodies. Samples were adjusted to equal protein amounts (30 μg for Flv2, Flv4 and Sll0218; 5 μg for PsaB, D1, Flv3, OCP and AtpB).

α-tocopherol biosynthesis [29]. α-Tocopherol functions as antioxidant [30] and could recently be demonstrated to protect D1 de novo synthesis during PSII repair in *Synechocystis* [31]. With the enhanced PsaB levels in mind (see Figs. 6 and 7), it was interesting to find the ORF *slr*0846 among the upregulated genes (2 fold). The encoded protein is an Rrf2-type transcriptional regulator that is required for proper light-dependent expression of *psaAB* in *Synechocystis* [32].

When we inspected the significantly downregulated genes we found as expected in Δ*fed7* the mutated gene *sll*0662 reduced (0.5 fold) in transcript abundance. Since we could not detect any full-length *fed7* transcript (Fig. 1) by RT-qPCR, we anticipate that the remaining signal arises from the DNA-microarray probe that binds to the region before the insertion site of the KmR cassette. A scheme showing the *fed7* ORF and the respective primer and microarray probe binding sites is given in Fig. A.1.

Intriguingly, the strongest alterations were observed for the genes of the *flv4–2* operon. In WT cells, these genes belong to the most upregulated genes after shift from HC to LC conditions [7,33]. In Δ*fed7* cells, the transcript levels of *sll*0217 (*flv4*), *sll*0218 and *sll*0219 (*flv2*) constituted only 25% and 42%, respectively, of the WT amount under LC conditions. Besides the *flv4–2* operon we identified several additional genes that are normally induced by C_i limiting conditions [7,33], such as *sll*1732 (*ndhF3*), *sll*0026 (*ndhF4*), genes of the *ndhD5* operon (*slr*2006-*slr*2012), or *sll*1032 (*ccmN*). While the *ndhF3* and *ndhF4* genes encode for specific subunits of NDH complexes involved in CO_2 uptake [34,35], the function of NdhD5 and NdhD6 remains unknown. CcmN is involved in the biogenesis of carboxysomes, the typical microcompartments in cyanobacteria specialized for efficient CO_2 fixation [36]. For all genes we found reduced transcript accumulation in the mutant, indicating incomplete induction of the characteristical LC response. It should be noted that also transcript levels of *slr*0947 were significantly reduced (0.64 fold) in the mutant. This gene encodes a regulator of phycobilisome association (RpaB) to the reaction centers of PSI and PSII, also known as Ycf27 [37].

In summary, the results indicate that Fed7 has impact on the transcriptional control of various components that are important in coping with LC and accompanying photooxidative stress conditions. Whether this impact is direct or rather a secondary effect remains to be investigated.

4. Discussion

Genomes of photosynthetic organisms contain multiple genes for Fed. The plant *Arabidopsis thaliana* contains six different *fed* genes [38], while the cyanobacterium *Synechocystis* has five ORFs encoding Fed. Importantly, besides these plant-type Fed *Synechocystis* and cyanobacteria in general also employ bacterial-type Fed, which typically contain [4Fe–4S] cluster as an active center, in contrast to [2Fe–2S] cluster in the plant-type Fed. It is a matter of debate whether this manifold Fed fulfill redundant or rather divergent functions (e.g. [38]). In this study we provide evidence that the bacterial-type Fed7 functions under photooxidative stress promoting conditions, such as LC and HL, as a regulator to organize distinct components of the acclimation response in *Synechocystis*.

Enhancement of *fed7* expression was observed under LC compared to HC conditions and was further fortified by concomitant increase in light intensity (Fig. 1). These environmental changes are known to induce photooxidative stress for cyanobacteria, due to the fact that cell metabolism cannot keep pace with photosynthetic light reactions resulting in imbalanced energy absorption versus consumption. Together with previous findings indicating that expression of *fed7* is induced by treatment with 3 mM H_2O_2 [4] as well as with a strong oxidant selenate [5], it is presumable that Fed7 is involved in coping not only with oxidative but also specifically with photooxidative stress.

To unravel the biological function of Fed7 in this process we generated a mutant strain by insertion of a kanamycin resistance cassette into the ORF. The gene *fed7* is part of an operon, and it was important to ensure that disruption of *fed7* does not affect the expression of the two upstream-situated genes of the operon, *ssl*1263 and *sll*0661 (*ycf35*) which encode still hypothetical proteins (Fig. 2A). Uninfluenced expression of both *ssl*1263 and *sll*0661, proven by microarray analysis of cells from standard growth conditions, was taken as an indication of normal expression of these genes despite elimination of *fed7*. It is intriguing to note that the operon structure is highly conserved throughout the cyanobacterial lineage including *Prochlorococcus* species with their strongly reduced genomes (see Cyanobase; http://genome.microbedb.jp/cyanobase), pointing to a basically important and concerted function of all three proteins encoded by the operon.

Despite the strict conservation of *fed7* in cyanobacterial genomes, the constructed Δ*fed7* mutant fully segregated (Fig. 2B) and showed unimpaired growth (Fig. A.2), demonstrating that Fed7 is not essential in *Synechocystis* under the tested conditions. Nevertheless, we observed distinct differences between WT and the mutant during physiological characterization of Δ*fed7*. Such differences were detected only at LC, and the effects were more pronounced in combination with HL, which is consistent with the transcriptional upregulation of *fed7* under LC [7] and HL conditions (Fig. 1) and the suggested functional significance of Fed7 at photooxidative stress.

Based on our results we suggest the following model (Fig. 8) for the regulatory role of Fed7 in promoting cell management with photooxidative stress.

When cyanobacteria are confronted with environmental changes, such as altered C_i concentrations and light intensities, they effectively respond by modifying expression of distinct gene sets (e.g. [7,33,39,40]). Under the photooxidative stress promoting conditions applied here, both C_i and light concentrations have to be quantified, integrated to trigger an adequate physiological response, and by this to avoid photooxidative stress. Besides a yet unknown LC signal [7,41,42], the light intensity is perceived and quantified as photosynthetic electron flow signal [43]. In accordance to the photosynthetic electron flow the plant-type Fed1 becomes reduced as terminal electron acceptor from PSI. As long as NADPH is consumed mainly in CO_2 fixation processes, $NADP^+$ is regenerated in the Calvin–Benson cycle and can be reduced

Table 2
List of genes with significantly increased transcript abundances in cells of Δ*fed7* mutant compared to WT 48 h after shift from HC to LC conditions. Expression values from three biological replicates were used for calculations and all genes with *q*-value below a threshold of false discovery rate 0.05 were selected as differentially expressed genes.

ORF	Gene name	Annotation acc. to Cyanobase	Δ*fed7*/WT (fold)	*q*-Value
sll0428		Unknown protein	4.14	0.020
slr0291		Hypothetical protein	3.94	0.023
sll1188		Hypothetical protein	3.68	0.047
sll0280		Unknown protein	3.12	0.024
slr0675		Unknown protein	3.10	0.026
ssr1251[a]		Hypothetical protein	2.51	0.019
slr1307		Hypothetical protein	2.48	0.050
slr0721		Malic enzyme	2.30	0.005
sll0381		Hypothetical protein	2.25	0.009
sml0010		Putative transposase	2.22	0.047
slr0750[a]	*chlN*	Light-independent protochlorophyllide reductase subunit ChlN	2.19	0.018
sll0283		Hypothetical protein	2.14	0.049
slr1826		Hypothetical protein	2.13	0.041
ssl0259		Hypothetical protein	2.13	0.009
sml0003	*psbM*	Photosystem II reaction center M protein	2.11	0.040
slr0846		Rrf2-type protein	2.04	0.044
sll1762		Periplasmic protein, putative polar amino acid transport system substrate-binding protein	2.00	0.030
sll1036		Hypothetical protein	1.96	0.048
slr0889		Hypothetical protein	1.96	0.029
slr0699		Unknown protein	1.92	0.036
slr2036		Putative transposase [ISY203a]	1.89	0.008
sll0284		Hypothetical protein	1.85	0.045
sll1712		DNA binding protein HU	1.78	0.015
slr1773		Unknown protein	1.77	0.004
slr1812		Hypothetical protein	1.75	0.036
ssl0769		Putative transposase	1.75	0.022
sll1365		Unknown protein	1.74	0.043
sll0622	*nadA*	Quinolinate synthetase	1.73	0.009
slr0226		Unknown protein	1.73	0.015
sll0828	*nylA*	Putative amidase	1.72	0.039
slr0016		Hypothetical protein	1.71	0.017
sll0832		Hypothetical protein	1.71	0.049
sll0985	*pamA*	Unknown protein	1.69	0.034
sll1584		Ferredoxin like protein	1.68	0.050
slr2042		Hypothetical protein	1.68	0.012
slr0579		Unknown protein	1.67	0.017
sll0179	*gltX*	Glutamyl-tRNA synthetase	1.65	0.038
slr0269		Hypothetical protein	1.61	0.012
slr1739	*psb28-2*	Photosystem II 13 kDa protein homolog	1.56	0.024
sll1888	*hik5*	Two-component sensor histidine kinase	1.55	0.010
sll0499		Hypothetical protein	1.55	0.029
sll1355		Hypothetical protein	1.53	0.030
slr0821		Hypothetical protein	1.46	0.031
sll1693		Hypothetical protein	1.45	0.043
slr0817	*entC*, *menF*	Salicylate biosynthesis isochorismate synthase	1.44	0.040
sll0781		Hypothetical protein	1.43	0.049
slr0818		Hypothetical protein	1.43	0.049
sll1426		Unknown protein	1.43	0.014
slr2060		Hypothetical protein	1.43	0.015
slr0185	*umpS*	Orotate phosphoribosyltransferase	1.41	0.041
sll1037		Unknown protein	1.41	0.017
sll0446		Unknown protein	1.39	0.043
slr1348	*cysE*, *cycE*	Serine acetyltransferase	1.38	0.023
slr1639	*smpB*	SsrA-binding protein	1.29	0.044

[a] The genes *slr*0749, *ssr*1251and *slr*0750 presumably form an operon. Since the *q*-value of *slr*0749 was >0.05, the 1.92 fold change was excluded from the table.

by FNR using Fed1 as electron donor. However, if CO_2 concentrations become limiting, such as under LC conditions, Fed1 starts using alternative electron acceptors and accordingly delivers electrons also to ferredoxin thioredoxin reductase (FTR [44]), which in turn reduces Fed7. In fact, Marteyn et al. [5] showed such interaction between *Synechocystis* Fed7 and FTR in vitro. Reduced Fed7 either transfers electrons to glutaredoxin Grx2 [5] or possibly to another yet unknown acceptor molecule, such as a redox dependent regulator protein. Though it is purely speculative, it is conceivable that this regulator protein acts as transcriptional regulator or interacts with unknown transcriptional regulator(s). Thereby, Fed7 possibly functions directly, or rather indirectly, as a redox-dependent regulator on transcriptional level to secure acclimation to photooxidative stress conditions. This process integrates several strategies (reviewed in [45]). Here we focus on those steps Fed7 is possibly involved in.

First, upon photooxidative stress the light-harvesting capacity becomes reduced to prevent absorption of excess light energy. This is mainly realized by decrease in Chl *a* content with concurrent downregulation of PSI and also PSII. The decrease in PSI amount is much more pronounced [46]. It was demonstrated that this protective downregulation is not caused by reduced transcription of PSI genes but by primary reduction of the Chl *a* content [47]. We anticipate that Fed7 likely functions as negative regulator for the *chlL*/*chlN* operon, which encodes the light-independent protochlorophillide oxidoreductase [28]. High levels of reduced Fed7 lead to decline in cellular Chl *a* content and thus help to avoid overexcitation pressure and consequent generation of reactive oxygen species (ROS). Furthermore, Fed7 enhances expression of the regulator of phycobilisome association RpaB [37]. RpaB is an essential response regulator in *Synechocystis* for photosynthesis regulation and acclimation to a variety of environmental changes. Originally it was

Table 3
List of genes with significantly reduced transcript abundances in cells of Δ*fed7* mutant compared to WT 48 h after shift from HC to LC conditions. Expression values from three biological replicates were used for calculations and all genes with *q*-value below a threshold of false discovery rate 0.05 were selected as differentially expressed genes.

ORF	Gene name	Annotation acc. to Cyanobase	Δ*fed7*/WT (fold)	*q*-Value
sll0217[a]	*flv4*	Flavoprotein	0.24	0.009
sll0218[a]		Hypothetical protein	0.26	0.018
sll1732	*ndhF3*	NADH dehydrogenase subunit 5	0.33	0.037
slr2078		Hypothetical protein	0.35	0.007
slr2043	*znuA*	Zinc transport system substrate-binding protein	0.40	0.040
sll0639		Hypothetical protein	0.42	0.004
slr2002	*cphA*	Cyanophycin synthetase	0.47	0.008
sll0068		Unknown protein	0.47	0.001
slr0293	*gcvP*	Glycine dehydrogenase	0.48	0.018
sll0267		Unknown protein	0.49	0.004
slr2007[2]	*ndhD5*	NADH dehydrogenase subunit 4	0.49	0.015
ssr3122		Hypothetical protein	0.50	0.012
slr1875	*exoD*	Hypothetical protein	0.50	0.018
sll0662	*fed7*	4Fe–4S type iron–sulfur protein	0.50	0.001
sll0689	*nhaS3*, *napA1*	Na^+/H^+ antiporter	0.51	0.037
sll1108	*surE*	Stationary-phase survival protein SurE homolog	0.52	0.002
slr1281	*ndhJ*	NADH dehydrogenase subunit I	0.52	0.048
sll1213	*wcaG*	GDP-fucose synthetase	0.54	0.027
sll1032	*ccmN*	Carbon dioxide concentrating mechanism protein CcmN	0.55	0.016
slr1351	*murF*, *mra*	UDP-N-acetylmuramoylalanyl-D-glutamyl-2 6-diaminopimelate--D-alanyl-D-alanine ligase	0.55	0.018
sll1906	*orf484*	Hypothetical protein	0.56	0.044
sll0711	*ipk*	Isopentenyl monophosphate kinase	0.57	0.004
sll0529		Hypothetical protein	0.57	0.020
sll1386		Hypothetical protein	0.57	0.010
ssl0410		Unknown protein	0.57	0.007
sll1293	*taxW2*	Unknown protein	0.58	0.032
sll1499	*glsF*, *gltS*	Ferredoxin-dependent glutamate synthase	0.59	0.008
slr1407		Unknown protein	0.60	0.032
slr0262		Unknown protein	0.62	0.005
slr2010[2]	*mrpE*	Hypothetical protein	0.62	0.026
slr0922	*PTH*	Peptidyl-tRNA hydrolase	0.63	0.050
slr0947	*rpaB*, *ycf27*	Response regulator for energy transfer	0.64	0.048
sll0649	*rre3*	Two-component response regulator OmpR subfamily	0.64	0.015
slr0665	*acnB*	Aconitate hydratase	0.64	0.046
slr1267	*ftsW*	Cell division protein FtsW	0.64	0.041
slr1044	*ctr1*, *taxD3*	Methyl-accepting chemotaxis protein	0.64	0.023
slr0559	*natB*	Periplasmic binding protein of ABC transporter	0.65	0.029
sll1540	*sed3*, *dpm1*	Dolichyl-phosphate-mannose synthase	0.65	0.015
slr1911		Hypothetical protein	0.67	0.018
slr2009[2]	*ndhD6*	NADH dehydrogenase subunit 4	0.67	0.019
slr2005		Periplasmic protein, function unknown	0.68	0.019
sll1060		Hypothetical protein	0.68	0.025
sll0482		Unknown protein	0.68	0.026
slr1331	*ymxG*	Periplasmic processing protease	0.70	0.048
slr1799		Hypothetical protein	0.71	0.034
sll1994	*hemB*	Porphobilinogen synthase	0.71	0.019
slr0765	*mscS*	Hypothetical protein	0.71	0.003
slr0014	*mgtC*	Mg^{2+} transport ATPase	0.71	0.034
sll1941	*gyrA*	DNA gyrase A subunit	0.72	0.028
slr0904	*comM*	Competence protein ComM homolog	0.72	0.015
slr1478		Hypothetical protein	0.72	0.032
sll0026	*ndhF4*	NADH dehydrogenase subunit 5	0.72	0.021
sll1019	*gloB*	Hydroxyacylglutathione hydrolase	0.73	0.041
sll0681	*pstC1*	Phosphate transport system permease protein PstC homolog	0.73	0.035
slr2011[2]	*mrpA*	Hypothetical protein	0.73	0.042
slr1508	*dgdA*, *KtrE*	Probable glycosyltransferase	0.73	0.034
sll1929	*comEC*	Competence protein ComE	0.74	0.021
sll0148		Hypothetical protein	0.75	0.026
slr0534	*slt*	Probable transglycosylase	0.75	0.040
sll0804		Hypothetical protein	0.75	0.041
slr1672	*glpK*	Glycerol kinase	0.75	0.036
sll0072		Hypothetical protein	0.75	0.025
slr0238		Hypothetical protein	0.77	0.036
sll1501	*cobB*, *cbiA*	Cobyrinic acid a,c-diamide synthase	0.77	0.045
slr1415		Hypothetical protein	0.78	0.040
slr1924	*pbp7*, *ampH*	D-alanyl-D-alanine carboxypeptidase	0.78	0.045
slr1563		Hypothetical protein	0.79	0.044
slr0415	*nhaS5*	Na^+/H^+ antiporter	0.79	0.046

Genes forming an operon are indicated with bold superscripted numbers.
[a] *sll*0217, *sll*0218 and *sll*0219 form the *flv4–2* operon. Since the *q*-value of *sll*0219 was >0.05, the 0.42 fold change was excluded from the table.

shown that RpaB controls uncoupling of phycobilisomes from PSII and thereby regulates distribution of absorbed light energy to the photosystems [37]. Later on it could be demonstrated that RpaB binds to the high light regulatory sequence and thus regulates HL stress responsive genes [48] and also PSI genes [49]. However, though we observed lower *rpaB* transcript levels in Δ*fed7* we could not detect any effect on state

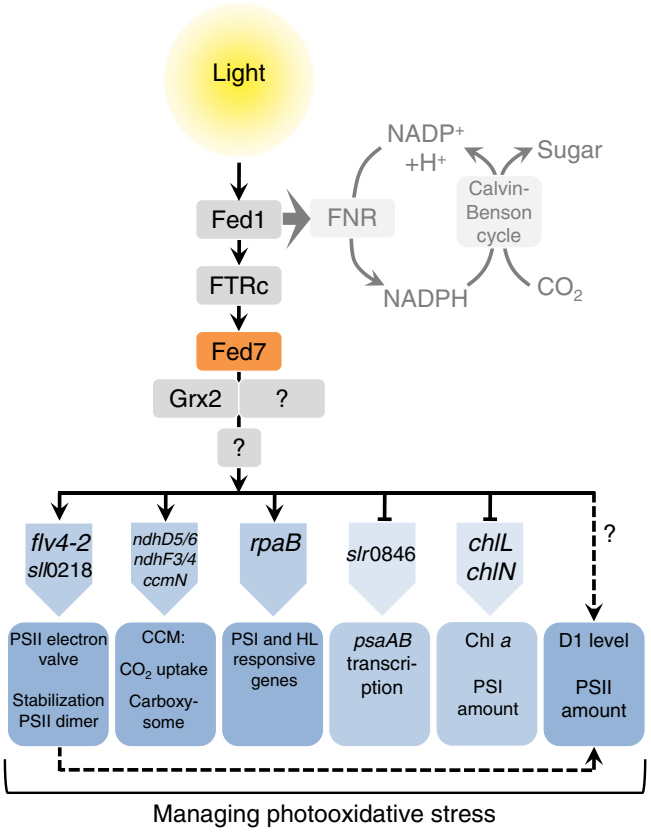

Fig. 8. Hypothetical model of the biological function of Fed7 under photooxidative stress conditions. Under LC and HL conditions NADPH is not sufficiently consumed by the Calvin–Benson cycle. To prevent acceptor limitation alternative electron sinks need to be recruited and photoprotective mechanisms activated. Probably, if NADPH usage is restricted, Fed1 does not pass electrons via FNR to $NADP^+$, but instead transfers electrons via ferredoxin–thioredoxin reductase catalytic chain (FTRc) to Fed7. Elevated levels of reduced Fed7 either directly or indirectly, via glutaredoxin 2 (Grx2) or other unknown proteins (?), enhances expression of the PSII electron valve Flv2/Flv4 (*flv4–2*) and the co-transcribed chaperone Sll0218 (*sll*0218), components of the CCM (*ndhD5/6*, *ndhF3/4*, *ccmN*), and the regulator of phycobilisome association (*rpaB*). As a result, dissipation of excitation energy by the PSII electron valve and stabilization of PSII dimers ensure adequate D1 level and functional PSII under photooxidative stress conditions. In contrast, Fed7 negatively affects expression of *chlL*, *chlN*, and *slr*0846, the transcriptional activator for *psaAB*. Thus, Chl *a* biosynthesis and PSI amounts get downregulated to avoid overexcitation and ROS generation, finally. For a more detailed description, see the text.

transitions (data not shown) or HL-responsive genes in the mutant. Besides RpaB we detected negative regulatory effect of Fed7 on expression of the transcriptional regulator Slr0846. This Rrf2-type protein acts as transcriptional activator for the PSI center protein genes *psaA* and *psaB* under low-light conditions [32]. Together with RpaB, the concerted action of both transcriptional regulators is crucial for correct HL-dependent repression of *psaAB*.

Second, upon photooxidative stress several mechanisms are induced to protect the photosynthetic apparatus. According to our data, Fed7 is involved in upregulation of the *flv4–2* operon. We recently demonstrated that Flv2 and Flv4 open up an alternative electron valve for PSII under photooxidative stress conditions, while the small thylakoid membrane protein Sll0218 encoded by the same operon stabilizes the PSII dimers [16,17]. Due to its delicate function, expression of the operon is tightly controlled on several levels including transcriptional regulators and antisense RNAs [50].

Third, photooxidative conditions reinforce C_i metabolism to consume reducing equivalents and thus to mitigate the acceptor side limitation of PSI and subsequent ROS generation. The cyanobacterial CCM employs proteinous microcompartments, the carboxysomes, and multiple energy-driven C_i uptake systems to allow efficient CO_2 fixation (reviewed in [41,51,52]). Several regulators of the LC-inducible regulon have been identified to date, such as CmpR [53], NdhR [33], or the AbrB-like protein Sll0822 [54]. Here we found evidence that Fed7 contributes to the controlled expression of distinct components of the CCM. Fed7 is needed for proper expression of the carboxysome biogenesis and shell protein CcmN [36]. Furthermore, Fed7 enhances transcription of *ndhF3* and *ndhF4*, which encode subunits of the LC-inducible and constitutive CO_2 uptake systems [34,35], respectively. Also genes of the *ndhD5* operon are affected by Fed7. However, the biological function of the encoded NdhD5 and NdhD6 proteins has not been identified yet.

When the Fed7 protein is missing, as in the case of the Δ*fed7* mutant, the cyanobacterial cells cannot properly respond to photooxidative stress conditions (LC + HL). Transcription of the Chl *a* biosynthesis genes *chlL*/*chlN* is upregulated in the mutant compared to WT (Table 2) and thus Δ*fed7* cells contain higher Chl *a* amounts (Fig. 3B, C) and accompanying increased PSI levels (Figs. 6 and 7, Table 1) than WT cells under LC and HL conditions. Therefore, Δ*fed7* cells are likely more susceptible to generation of detrimental ROS. Expression of the *flv4–2* operon is not fully induced in Δ*fed7* (see reduced transcript amounts (Table 2) and reduced protein amounts (Fig. 7)) with the consequence that the Flv2–4 mediated photoprotection is not fully active under the used photooxidative stress conditions. Additionally, the mutant fails to properly enhance the expression of all CCM genes (Table 2). In summary, different acclimatory components that should enable the cells to deal with photooxidative stress are deregulated. To compensate for the imperfect protection repertoire, several other components are upregulated such as carotenoid accumulation (Fig. 3B, C) and biosynthesis of the antioxidant α-tocopherol (Table 2). We did not find any evidence for a regulatory effect of Fed7 on OCP, which also contributes as a quenching molecule to photoprotection in cyanobacteria [27,55]. Eventually, compensatory reactions, such as the antioxidant accumulation allow the mutant to grow as fast as the WT, yet with some deviations. For an unknown reason, the D1 amounts (Figs. 6, 7 and Fig. A.5), PSII levels (Fig. 5) and finally also the PSII activity (Fig. 4C, D, F, Table 1) are diminished in Δ*fed7* under photooxidative stress conditions. It is conceivable, that the low level of Sll0218 (Fig. 7) might cause the observed PSII malfunction, since the Sll0218 protein functions as stabilizing chaperone for the PSII dimer under LC conditions [17].

In the context of our study it is important to mention that very recently, the function of the hypothetical chloroplast ORF Ycf34 was investigated in *Synechocystis*. Like Fed7, also Ycf34 contains a [4Fe–4S] cluster and interacts with the photosynthetic electron transfer chain. In contrast to Fed7, Ycf34 is proposed to function in redox signaling under low light conditions [56].

Bacterial-type Fed as single proteins are not conserved in the green lineage. Intriguingly, Fed-like proteins were found as distinct domains in chloroplast DnaJ-like (CDJ) proteins in the green alga *Chlamydomonas reinhardtii* [57]. According to our analysis (Fig. A.6), Fed7 is the closest homolog to this Fed domain in *Synechocystis*. A recent phylogenetic study [58] revealed that indeed the Fed domain is of cyanobacterial origin and acquired by photosynthetic eukaryotes through horizontal gene transfer. Very likely, the fusion of the Fed to the J-domain happened after the branching into Glaucophyta, Rhodophyta and Viridiplantae but before the differentiation within the Viridiplantae since only members of Viridiplantae contain CDJ proteins [58]. In *Chlamydomonas* the CDJ3–5 proteins were postulated to function as redox switches for interaction with HSP70B [57]. HSP70B is the major chloroplast HSP70 chaperone in *Chlamydomonas* and assists in the repair of photodamaged D1 to prevent photoinhibition [59]. Thus CDJ3–5 proteins exert as co-chaperones of HSP70B a light-dependent regulatory function in protection of PSII [57]. Importantly, CDJ proteins are not only restricted to green algae but also exist in higher plants such as *Arabidopsis thaliana* (AT2G42750, AT3G05345, AT5G23240, see Fig. A.6 [5,57]). We suggest that the function of Fed7 evolved from a regulator specialized bacterial-type Fed in cyanobacteria to a composite

protein, which consists of a redox-regulatory switch fused to a DnaJ-like protein in chloroplasts of Viridiplantae.

Acknowledgements

This work was supported by the Academy of Finland, project numbers 133299 (M. E.) 118637 and 271832 (E.M.A.), the Finnish Doctoral Programme in Computational Chemistry and Molecular Spectroscopy (LasKeMo) (H.M.), and the EU 7th FP ENERGY Project Energy-2010-1 Agreement 256808. We thank the Finnish DNA Microarray and Sequencing Centre (Turku, Finland) for assistance with the microarray analyses.

Appendix A. Supplementary data

Supplementary data to this article can be found online at http://dx.doi.org/10.1016/j.bbabio.2014.04.006.

References

[1] M. Poncelet, C. Cassier-Chauvat, X. Leschelle, H. Bottin, F. Chauvat, Targeted deletion and mutational analysis of the essential (2Fe–2S) plant-like ferredoxin in *Synechocystis* PCC6803 by plasmid shuffling, Mol. Microbiol. 28 (1998) 813–821.
[2] J. Van der Plas, R. De Groot, M. Woortman, F. Cremers, M. Borrias, G. Van Arkel, P. Weisbeek, Genes encoding ferredoxins from *Anabaena* sp. PCC 7937 and *Synechococcus* sp. PCC 7942: structure and regulation, Photosynth. Res. 18 (1988) 179–204.
[3] G.T. Hanke, Y. Satomi, K. Shinmura, T. Takao, T. Hase, A screen for potential ferredoxin electron transfer partners uncovers new, redox dependent interactions, Biochim. Biophys. Acta 1814 (2011) 366–374.
[4] K. Mazouni, F. Domain, F. Chauvat, C. Cassier-Chauvat, Expression and regulation of the crucial plant-like ferredoxin of cyanobacteria, Mol. Microbiol. 49 (2003) 1019–1029.
[5] B. Marteyn, F. Domain, P. Legrain, F. Chauvat, C. Cassier-Chauvat, The thioredoxin reductaseglutaredoxins–ferredoxin crossroad pathway for selenate tolerance in *Synechocystis* PCC6803, Mol. Microbiol. 71 (2009) 520–532.
[6] A. Bateman, L. Coin, R. Durbin, R.D. Finn, V. Hollich, S. Griffiths-Jones, A. Khanna, M. Marshall, S. Moxon, E.L. Sonnhammer, D.J. Studholme, C. Yeats, S.R. Eddy, The Pfam protein families database, Nucleic Acids Res. 32 (2004) D138–D141.
[7] M. Eisenhut, E.A. von Wobeser, L. Jonas, H. Schubert, B.W. Ibelings, H. Bauwe, H.C. Matthijs, M. Hagemann, Long-term response toward inorganic carbon limitation in wild type and glycolate turnover mutants of the cyanobacterium *Synechocystis* sp. strain PCC 6803, Plant Physiol. 144 (2007) 1946–1959.
[8] M.A. Hernández-Prieto, V. Schön, J. Georg, L. Barreira, J. Varela, W.R. Hess, M.E. Futschik, Iron deprivation in *Synechocystis*: inference of pathways, non-coding RNAs, and regulatory elements from comprehensive expression profiling, G3 (Bethesda) 2 (2012) 1475–1495.
[9] A.K. Singh, L.M. McIntyre, L. Sherman, Microarray analysis of the genome-wide response to iron deficiency and iron reconstitution in the cyanobacterium *Synechocystis* sp. PCC 6803, Plant Physiol. 132 (2003) 1825–1839.
[10] R. Rippka, J. Deruelles, J.B. Waterbury, M. Herdman, R.Y. Stanier, Generic assignments, strain histories and properties of pure cultures of cyanobacteria, J. Gen. Microbiol. 111 (1979) 1–16.
[11] M. Eisenhut, S. Kahlon, D. Hasse, R. Ewald, J. Lieman-Hurwitz, T. Ogawa, W. Ruth, H. Bauwe, A. Kaplan, M. Hagemann, The plant-like C2 glycolate cycle and the bacterial-like glycerate pathway cooperate in phosphoglycolate metabolism in cyanobacteria, Plant Physiol. 142 (2006) 333–342.
[12] T. Tyystjärvi, M. Herranen, E.-M. Aro, Regulation of translation elongation in cyanobacteria: membrane targeting of the ribosome nascent-chain complexes controls the synthesis of D1 protein, Mol. Microbiol. 40 (2001) 476–484.
[13] M. Pollari, V. Ruotsalainen, S. Rantamäki, E. Tyystjärvi, T. Tyystjärvi, Simultaneous inactivation of sigma factors B and D interferes with light acclimation of the cyanobacterium *Synechocystis* sp. strain PCC 6803, J. Bacteriol. 191 (2009) 3992–4001.
[14] J.M. Ruijter, C. Ramakers, W.M.H. Hoogaars, Y. Karlen, O. Bakker, M.J.B. van den Hoff, A.F.M. Moorman, Amplification efficiency: linking baseline and bias in the analysis of quantitative PCR data, Nucleic Acids Res. 37 (2009) e45.
[15] C.I. Sicora, S.E. Appleton, C.M. Brown, J. Chung, J. Chandler, et al., Cyanobacterial psbA families in *Anabaena* and *Synechocystis* encode trace, constitutive and UVB-induced D1 isoforms, Biochim. Biophys. Acta 1757 (2006) 47–56.
[16] P. Zhang, Y. Allahverdiyeva, M. Eisenhut, E.-M. Aro, Flavodiiron proteins in oxygenic photosynthetic organisms: photoprotection of photosystem II by Flv2 and Flv4 in *Synechocystis* sp. PCC 6803, PLoS One 4 (2009) e5331.
[17] P. Zhang, M. Eisenhut, A.M. Brandt, D. Carmel, H.M. Silén, I. Vass, Y. Allahverdiyeva, T.A. Salminen, E.M. Aro, Operon flv4-flv2 provides cyanobacterial photosystem II with flexibility of electron transfer, Plant Cell 24 (2012) 1952–1971.
[18] M. Kügler, L. Jänsch, V. Kruft, U.K. Schmitz, H.P. Braun, Analysis of the chloroplast protein complexes by blue-native polyacrylamide gel electrophoresis (BN-PAGE), Photosynth. Res. 53 (1997) 35–44.
[19] M. Herranen, N. Battchikova, P. Zhang, A. Graf, S. Sirpiö, V. Paakkarinen, E.M. Aro, Towards functional proteomics of membrane protein complexes in *Synechocystis* sp. PCC 6803, Plant Physiol. 134 (2004) 470–481.
[20] P. Zhang, C.I. Sicora, N. Vorontsova, Y. Allahverdiyeva, N. Battchikova, P.J. Nixon, E.M. Aro, FtsH protease is required for induction of inorganic carbon acquisition complexes in *Synechocystis* sp. PCC 6803, Mol. Microbiol. 65 (2007) 728–740.
[21] C. Vernotte, M. Picaud, D. Kirilovsky, J. Olive, G. Ajlani, C. Astier, Changes in the photosynthetic apparatus in the cyanobacterium *Synechocystis* sp. PCC 6714 following light-to-dark and dark-to-light transitions, Photosynth. Res. 32 (1992) 45–57.
[22] Y. Allahverdiyeva, M. Ermakova, M. Eisenhut, P. Zhang, P. Richaud, M. Hagemann, L. Cournac, E.M. Aro, Interplay between flavodiiron proteins and photorespiration in *Synechocystis* sp. PCC 6803, J. Biol. Chem. 286 (2011) 24007–24014.
[23] Y. Allahverdiyeva, H. Mustila, M. Ermakova, L. Bersanini, P. Richaud, G. Ajlani, N. Battchikova, L. Cournac, E.M. Aro, Flavodiiron proteins Flv1 and Flv3 enable cyanobacterial growth and photosynthesis under fluctuating light, Proc. Natl. Acad. Sci. U. S. A. 110 (2013) 4111–4116.
[24] Y. Helman, D. Tchernov, L. Reinhold, M. Shibata, T. Ogawa, R. Schwarz, I. Ohad, A. Kaplan, Genes encoding A-type flavoproteins are essential for photoreduction of O_2 in cyanobacteria, Curr. Biol. 13 (2003) 230–235.
[25] C. Hackenberg, A. Engelhardt, H.C. Matthijs, F. Wittink, H. Bauwe, A. Kaplan, M. Hagemann, Photorespiratory 2-phosphoglycolate metabolism and photoreduction of O_2 cooperate in high-light acclimation of *Synechocystis* sp. strain PCC 6803, Planta 230 (2009) 625–637.
[26] A. Wilson, G. Ajlani, J.M. Verbavatz, I. Vass, C.A. Kerfeld, D. Kirilovsky, A soluble carotenoid protein involved in phycobilisome-related energy dissipation in cyanobacteria, Plant Cell 18 (2006) 992–1007.
[27] D. Kirilovsky, Photoprotection in cyanobacteria: the orange carotenoid protein (OCP)-related non-photochemical-quenching mechanism, Photosynth. Res. 93 (2007) 7–16.
[28] Q. He, D. Brune, R. Nieman, W. Vermaas, Chlorophyll alpha synthesis upon interruption and deletion of por coding for the light-dependent NADPH: protochlorophyllide oxidoreductase in a photosystem-I-less/chlL$^-$ strain of *Synechocystis* sp. PCC 6803, Eur. J. Biochem. 1 (1998) 161–172.
[29] D. Dähnhardt, J. Falk, J. Appel, T.A. van der Kooij, R. Schulz-Friedrich, K. Krupinska, The hydroxyphenylpyruvate dioxygenase from *Synechocystis* sp. PCC 6803 is not required for plastoquinone biosynthesis, FEBS Lett. 17 (2002) 177–181.
[30] H. Maeda, Y. Sakuragi, D.A. Bryant, D. DellaPenna, Tocopherols protect *Synechocystis* sp. strain PCC 6803 from lipid peroxidation, Plant Physiol. 138 (2005) 1422–1435.
[31] S. Inoue, K. Ejima, E. Iwai, H. Hayashi, J. Appel, E. Tyystjärvi, N. Murata, Y. Nishiyama, Protection by α-tocopherol of the repair of photosystem II during photoinhibition in *Synechocystis* sp. PCC 6803, Biochim. Biophys. Acta 1807 (2011) 236–241.
[32] T. Midorikawa, K. Matsumoto, R. Narikawa, M. Ikeuchi, An Rrf2-type transcriptional regulator is required for expression of psaAB genes in the cyanobacterium *Synechocystis* sp. PCC 6803, Plant Physiol. 151 (2009) 882–892.
[33] H.L. Wang, B.L. Postier, R.L. Burnap, Alterations in global patterns of gene expression in *Synechocystis* sp. PCC 6803 in response to inorganic carbon limitation and the inactivation of ndhR, a LysR family regulator, J. Biol. Chem. 279 (2004) 5739–5751.
[34] M. Shibata, H. Ohkawa, T. Kaneko, H. Fukuzawa, S. Tabata, A. Kaplan, T. Ogawa, Distinct constitutive and low-CO_2-induced CO_2 uptake systems in cyanobacteria: genes involved and their phylogenetic relationship with homologous genes in other organisms, Proc. Natl. Acad. Sci. U. S. A. 98 (2001) 11789–11794.
[35] P. Zhang, N. Battchikova, T. Jansen, J. Appel, T. Ogawa, E.M. Aro, Expression and functional roles of the two distinct NDH-1 complexes and the carbon acquisition complex NdhD3/NdhF3/CupA/Sll1735 in *Synechocystis* sp PCC 6803, Plant Cell 16 (2004) 3326–3340.
[36] J.N. Kinney, A. Salmeen, F. Cai, C.A. Kerfeld, Elucidating essential role of conserved carboxysomal protein CcmN reveals common feature of bacterial microcompartment assembly, J. Biol. Chem. 287 (2012) 17729–17736.
[37] M.K. Ashby, C.W. Mullineaux, Cyanobacterial ycf27 gene products regulate energy transfer from phycobilisomes to photosystems I and II, FEMS Microbiol. Lett. 181 (1999) 253–260.
[38] G. Hanke, P. Mulo, Plant type ferredoxins and ferredoxin-dependent metabolism, Plant Cell Environ. 36 (2013) 1071–1084.
[39] Y. Hihara, A. Kamei, M. Kanehisa, A. Kaplan, M. Ikeuchi, DNA microarray analysis of cyanobacterial gene expression during acclimation to high light, Plant Cell 13 (2001) 793–806.
[40] J. Mitschke, J. Georg, I. Scholz, C.M. Sharma, D. Dienst, J. Bantscheff, B. Voss, C. Steglich, A. Wilde, J. Vogel, W.R. Hess, An experimentally anchored map of transcriptional start sites in the model cyanobacterium *Synechocystis* sp. PCC6803, Proc. Natl. Acad. Sci. U. S. A. 108 (2011) 2124–2129.
[41] A. Kaplan, L. Reinhold, CO_2 concentrating mechanisms in photosynthetic microorganisms, Annu. Rev. Plant Physiol. Plant Mol. Biol. 50 (1999) 539–570.
[42] F.J. Woodger, M.R. Badger, G.D. Price, Sensing of inorganic carbon limitation in *Synechococcus* PCC7942 is correlated with the size of the internal inorganic carbon pool and involves oxygen, Plant Physiol. 139 (2005) 1959–1969.
[43] C.W. Mullineaux, How do cyanobacteria sense and respond to light? Mol. Microbiol. 41 (2001) 965–971.
[44] S. Dai, R. Friemann, D.A. Glauser, F. Bourquin, W. Manieri, P. Schürmann, H. Eklund, Structural snapshots along the reaction pathway of ferredoxin–thioredoxin reductase, Nature 448 (2007) 92–96.
[45] M. Muramatsu, Y. Hihara, Acclimation to high-light conditions in cyanobacteria: from gene expression to physiological responses, J. Plant Res. 125 (2012) 11–39.
[46] J. Kopecná, J. Komenda, L. Bucinská, R. Sobotka, Long-term acclimation of the cyanobacterium *Synechocystis* sp. PCC 6803 to high light is accompanied by an enhanced production of chlorophyll that is preferentially channeled to trimeric photosystem I, Plant Physiol. 160 (2012) 2239–2250.

[47] M. Muramatsu, K. Sonoike, Y. Hihara, Mechanism of downregulation of photosystem I content under high-light conditions in the cyanobacterium *Synechocystis* sp. PCC 6803, Microbiol. 155 (2009) 989–996.
[48] A.D. Kappell, L.G. van Waasbergen, The response regulator RpaB binds the high light regulatory 1 sequence upstream of the high-light-inducible hliB gene from the cyanobacterium Synechocystis PCC 6803, Arch. Microbiol. 187 (2007) 337–342.
[49] Y. Seino, T. Takahashi, Y. Hihara, The response regulator RpaB binds to the upstream element of photosystem I genes to work for positive regulation under low-light conditions in *Synechocystis* sp. strain PCC 6803, J. Bacteriol. 191 (2009) 1581–1586.
[50] M. Eisenhut, J. Georg, S. Klähn, I. Sakurai, H. Mustila, P. Zhang, W.R. Hess, E.M. Aro, The antisense RNA As1_flv4 in the cyanobacterium *Synechocystis* sp. PCC 6803 prevents premature expression of the flv4–2 operon upon shift in inorganic carbon supply, J. Biol. Chem. 287 (2012) 33153–33162.
[51] M.R. Badger, G.D. Price, B.M. Long, F.J. Woodger, The environmental plasticity and ecological genomics of the cyanobacterial CO_2 concentrating mechanism, J. Exp. Bot. 57 (2006) 249–265.
[52] G.D. Price, M.R. Badger, F.J. Woodger, B.M. Long, Advances in understanding the cyanobacterial CO_2-concentrating-mechanism (CCM): functional components, Ci transporters, diversity, genetic regulation and prospects for engineering into plants, J. Exp. Bot. 59 (2008) 1441–1461.
[53] T. Omata, S. Gohta, Y. Takahashi, Y. Harano, S. Maeda, Involvement of a CbbR homolog in low CO_2-induced activation of the bicarbonate transporter operon in cyanobacteria, J. Bacteriol. 183 (2001) 1891–1898.
[54] J. Lieman-Hurwitz, M. Haimovich, G. Shalev-Malul, A. Ishii, Y. Hihara, A. Gaathon, M. Lebendiker, A. Kaplan, A cyanobacterial AbrB-like protein affects the apparent photosynthetic affinity for CO_2 by modulating low-CO_2-induced gene expression, Environ. Microbiol. 11 (2009) 927–936.
[55] C. Boulay, L. Abasova, C. Six, I. Vass, D. Kirilovsky, Occurrence and function of the orange carotenoid protein in photoprotective mechanisms in various cyanobacteria, Biochim. Biophys. Acta 1777 (2008) 1344–1354.
[56] T. Wallner, Y. Hagiwara, G. Bernát, R. Sobotka, E.J. Reijerse, N. Frankenberg-Dinkel, A. Wilde, Inactivation of the conserved open reading frame ycf34 of *Synechocystis* sp. PCC 6803 interferes with the photosynthetic electron transport chain, Biochim. Biophys. Acta 1817 (2012) 2016–2026.
[57] K.V. Dorn, F. Willmund, C. Schwarz, C. Henselmann, T. Pohl, B. Hess, D. Veyel, B. Usadel, T. Friedrich, J. Nickelsen, M. Schroda, Chloroplast DnaJ-like proteins 3 and 4 (CDJ3/4) from *Chlamydomonas reinhardtii* contain redox-active Fe–S clusters and interact with stromal HSP70B, Biochem. J. 427 (2010) 205–215.
[58] C. Petitjean, D. Moreira, P. López-García, C. Brochier-Armanet, Horizontal gene transfer of a chloroplast DnaJ-Fer protein to Thaumarchaeota and the evolutionary history of the DnaK chaperone system in Archaea, BMC Evol. Biol. 12 (2012) 226.
[59] H. Heide, A. Nordhues, F. Drepper, S. Nick, M. Schulz-Raffelt, W. Haehnel, M. Schroda, Application of quantitative immunoprecipitation combined with knockdown and cross-linking to *Chlamydomonas* reveals the presence of vesicle-inducing protein in plastids 1 in a common complex with chloroplast HSP90C, Proteomics 9 (2009) 3079–3089.